Stokes' second problem with wall suction for upper convected Maxwell fluids

D. O. A. Cruz[1] e F. T. Pinho[2,3]

[1]Universidade Federal do Pará, Departamento de Engenharia Mecânica, Campus Universitário do Guamá, 66075-900 Belém, Pará, Brasil
email: doac@ufpa.br http://www.ufpa.br
[2] Faculdade de Engenharia da Universidade do Porto, Centro de Estudos de Fenómenos de Transporte, Rua Dr. Roberto Frias, s/n, 4200-465 Porto, Portugal
email: fpinho@fe.up.pt http://www.fe.up.pt
[3] Universidade de Minho, Largo do Paço, 4704-573 Braga, Portugal

Abstract

An analytical solution is derived for the time-dependent flow driven by the oscillation of a porous plate in an infinite viscoelastic fluid medium represented by the upper convected Maxwell model and in the presence of suction. Whereas for a Newtonian fluid there is a solution regardless of the amount of suction, for viscoelasticy the solution breaks down when the suction velocity exceeds the shear wave speed. The effects of suction, Reynolds number and fluid elasticity on the oscillating flow and its characteristic lengths are analysed in depth.

Keywords: *Stokes' second problem, Upper convected Maxwell fluid, wall suction, viscoelasticity*

1 Introduction

The time-dependent flow of viscoelastic fluids caused by the oscillation of a flat plate is of considerable interest both industrially as well as a test case to assess the performance of numerical methods for the computation of transient flows. As demonstrated by Oliveira [1], the performance of time discretization numerical methods needs to be assessed not only against start-up flows, but especially against unsteady flows of unlimited duration in order to better assess the accuracy of the methods and the propagation of errors over time.

A fundamental viscoelastic constitutive equation is the Upper Convected Maxwell fluid, UCM, which models the polymer contribution of some types of Boger fluids [2] and polymer melts of constant viscosity. The solution of Stokes' second problem for this fluid has been addressed recently by Hayat et al [3] and Aksel et al [4], using Fourier series. The start-up Poiseuille flow for the Oldroyd-B fluid was derived by Waters and King [5] for a pipe and by Mochimaru [6] for the flow between parallel plates. Regarding the plate bounded by an infinite body of fluid, Tanner [7] worked on Stokes' first problem for Oldroyd-B fluids and showed that for UCM fluids the shear waves propagated from the plate at a constant speed $c = \sqrt{\eta/(\rho\lambda)}$, where η, ρ and λ represent the viscosity coefficient, the density and relaxation time of the fluid, respectively. The solutions of Hayat et al [3] and Aksel et al [4] for Stokes' second problem include also the start-up from rest of the periodic oscillating flow, pioneered by Erdogan [8] for Newtonian fluids.

Given the nonlinear nature of the UCM viscoelastic constitutive equation ando f the advective term of the momentum equation, the solution of Stokes' second problem with suction through a porous wall is not simply the linear combination of the two simpler solutions, although the non-linearity in the momentum equation can be eliminated by consideration of a constant suction velocity. The solution of this more complex flow is not available in the literature for viscoelastic fluids and it is the objective of this work. The paper presents the theoretical solution for the flow of an UCM fluid resulting from the combination of a sinusoidal tangential oscillation of the wall with constant flow suction through the plate.

The paper is organized as follows. Section 2 presents the governing equations and the corresponding boundary and initial conditions. The analytical solution is obtained in Section 3 and the paper discusses some interesting results in Section 4, prior to the closure of this work.

2 Governing equations and boundary conditions

The flow under consideration is created by a plate perpendicular to the *y* –axis, oscillating in the *x*- direction and there is fluid in the region *y*≥ 0. Through the porous plate there is a constant time-independent suction velocity v_w ($v_w < 0$). The equations will be presented in normalized form for which the following scales are used: the characteristic velocity is the amplitude of the velocity oscillation of the plate (U_0); the characteristic length is U_0/ω, where ω is the frequency of oscillation of the plate, time is normalized as ωt and the stresses are normalized by $\eta_p\omega$, where η_p stands for the polymer viscosity coefficient. The normalization of the equations gives rise to the Reynolds (*Re*) and Deborah (*De*) numbers, which are defined as $\mathrm{Re} = \rho U_0^2/(\omega\eta_p)$ and $De = \lambda\omega$, respectively, with λ being the relaxation time of the polymer. Other dependent non-dimensional quantities help understand the flow physics and are introduced next.

The propagation of shear waves in elastic fluids takes place at a well defined velocity, [7] $c = \sqrt{\eta_p/(\rho\lambda)}$, leading to the definition of an elastic Mach number (*M*), the ratio of the characteristic velocity to the wave speed given by $M = \sqrt{Re \times De}$. Another non-dimensional parameter is the elasticity number (*E*), which has several interpretations (see chapter 7 in Joseph [9]). *E* is defined as the ratio between the Deborah and Reynolds numbers ($E = De/\mathrm{Re}$) and can be viewed as the ratio of elastic to viscous forces, as the square of the ratio of diffusion to wave velocities as well as the square of the ratio of two lengths over a relaxation time period, namely the diffusion length and the length traveled by shear waves. Finally, suction for viscoelastic fluids can alternatively be quantified by the suction elastic Mach number ($M_w \equiv v_w/c = v_w \times \sqrt{\mathrm{Re}\times De}$) instead of by the normalized suction velocity v_w. The relevance of M_w is clear as it naturally arises from the equations.

The normalised momentum equation for this unsteady flow is

$$\frac{\partial u}{\partial t} + v_w \frac{\partial u}{\partial y} = \frac{1}{Re}\frac{\partial \tau_{xy,p}}{\partial y} \tag{1}$$

with the polymer shear stress ($\tau_{yx} = \tau_{xy}$) given by the UCM differential constitutive equation (2) written in index notation and in non-dimensional form.

$$\tau_{ij,p} + De\left(\frac{\partial \tau_{ij,p}}{\partial t} + u_k \frac{\partial \tau_{ij,p}}{\partial x_k} - \tau_{jk,p}\frac{\partial u_i}{\partial x_k} - \tau_{ik,p}\frac{\partial u_j}{\partial x_k}\right) = \frac{\partial u_i}{\partial x_j} + \frac{\partial u_j}{\partial x_k}. \tag{2}$$

Equation (2) simplifies to the following set, where for convenience the subscript *p* has been dropped.

$$De\left(\frac{\partial \tau_{xy}}{\partial t} + v_w \frac{\partial \tau_{xy}}{\partial y} - \frac{\partial u}{\partial y}\tau_{yy}\right) + \tau_{xy} = \frac{\partial u}{\partial y} \tag{3-a}$$

$$De\left(\frac{\partial \tau_{yy}}{\partial t} + v_w \frac{\partial \tau_{yy}}{\partial y}\right) + \tau_{yy} = 0 \tag{3-b}$$

$$De\left(\frac{\partial \tau_{xx}}{\partial t} + v_w \frac{\partial \tau_{xx}}{\partial y} - 2\frac{\partial u}{\partial y}\tau_{xy}\right) + \tau_{xx} = 0 \tag{3-c}$$

This is further simplified by the assumption made here that $\tau_{yy} = 0$ is a solution of equation (3-b) as in steady Couette flow. The equations to be solved are subject to the following boundary and initial conditions: at $y = 0$, $u(0,t) = e^{D+it}$, at $y = \infty$, $u(\infty,t) = 0$ and at $t < 0$, $u(y,t) = 0$.

3 Analytical solution

The second assumption made here is that $u = u(\phi)$, $\tau_{xx} = \tau_{xx}(\phi)$ and $\tau_{xy} = \tau_{xy}(\phi)$, where $\phi = At + By$. Then, Equations (1), (2), (3-a) and (3-c) become Equations (4-a) to (4-c).

$$(A + v_w B)\frac{du}{d\phi} = \frac{B}{Re}\frac{d\tau_{xy}}{d\phi} \tag{4-a}$$

$$De(A + v_w B)\frac{d\tau_{xy}}{d\phi} + \tau_{xy} = B\frac{du}{d\phi} \tag{4-b}$$

$$De\left[\left(A+v_wB\right)\frac{d\tau_{xx}}{d\phi}-2B\frac{du}{d\phi}\tau_{xy}\right]+\tau_{xx}=0 \tag{4-c}$$

Using equation (4-b) to eliminate $du/d\phi$ in equation (4-a) and rearranging provides the following differential equation for τ_{xy}

$$\left[De\left(A+v_wB\right)-\frac{B^2}{Re\left(A+v_wB\right)}\right]\frac{d\tau_{xy}}{d\phi}+\tau_{xy}=0 \tag{5}$$

Defining $1/\alpha = A+v_wB$ and making $1/z = De\left(A+v_wB\right)-B^2/\left[Re\left(A+v_wB\right)\right] = De/\alpha-\alpha B^2/Re$, the integration of equation (5) provides the shear stress distribution of equation (6), where c_1 is to be determined later from a boundary condition.

$$\tau_{xy}=e^{-z\phi+c_1} \tag{6}$$

This shear stress and its derivative are back-substituted into equation (4-a), which provides the velocity derivative ($du/d\phi$) and the velocity distribution after integration, as follows:

$$\frac{du}{d\phi}=\frac{B}{Re\left(A+v_wB\right)}\left(-z\right)e^{-z\phi+c_1}\rightarrow u=\frac{B}{Re\left(A+v_wB\right)}e^{-z\phi+c_1}+c_2=\frac{B\alpha}{Re}e^{-z\phi+c_1}, \tag{7}$$

where $c_2=0$ on account of the boundary condition $u\left(\infty,t\right)=0$.

To obtain a differential equation on the normal stress τ_{xx} , $du/d\phi$ from equation (7) and τ_{xy} from equation (6) are substituted into equation (4-c) and rearranged to give

$$\frac{De}{\alpha}\frac{d\tau_{xx}}{d\phi}+\tau_{xx}=\left(-2z\right)\frac{DeB^2\alpha}{Re}e^{-2z\phi+2c_1} \tag{8}$$

Multiplying by $\exp\left(\alpha\phi/De\right)$ gives

$$\frac{d}{d\phi}\left(e^{\frac{\alpha}{De}\phi}\tau_{xx}\right)=\left(-2z\right)\frac{B^2\alpha^2}{Re}e^{\phi\left(-2z+\frac{\alpha}{De}\right)+2c_1} \tag{9}$$

and integrating provides the normal stress distribution

$$\tau_{xx}=\Gamma e^{-2z\phi+2c_1}+c_3e^{-\frac{\alpha}{De}\phi}\ \text{with}\ \Gamma=\left(-2z\right)\frac{DeB^2\alpha^2}{Re\left(\alpha\text{ - }2zDe\right)} \tag{10}$$

The first term on the right-hand-side of equation (10) is $\Gamma\tau_{xy}^2$, whereas the second term must vanish when $t\rightarrow\infty$. The solution remains valid in the absence of suction and this helps helps to define the general quantities *A* and *B* introduced earlier. At the wall the general velocity profile of Equation (7) only has a real component and it must be consistent with the no-slip condition. Hence, this equality at $y=0$ gives

$$\frac{B}{Re\left(A+v_wB\right)}e^{c_1}e^{-zAt}=e^De^{it} \tag{11}$$

from which two results are obtained: (1) the constant of integration c_1

$$c_1=D+\ln\left[\frac{Re\left(A+v_wB\right)}{B}\right] \tag{12}$$

and (2) the equality $-zA=i$

$$-zA=i\rightarrow\frac{-A}{De\left(A+v_wB\right)-\frac{B^2}{Re\left(A+v_wB\right)}}=i\ . \tag{13}$$

This is an algebraic second order equation on *B*, that can be solved to provide two possible solutions ($m=\pm1$).

$$B=\frac{Av_wRe\left(i\text{ - }2De\right)+mAi\sqrt{Re}\sqrt{v_w^2Re+4\left(i\text{ - }De\right)}}{2\left(v_w^2DeRe-1\right)}\ \text{with}\ m=\pm1. \tag{14-a}$$

It is clear that there is a singularity when $v_w^2DeRe=1$ (from its definition this corresponds to $M_w=-1$). For this particular viscoelastic case, Equation (13) turns out to be linear on *B* and its solution is

$$B=\frac{-A\left(1-iDe\right)\left(1+i2De\right)}{v_w^*\left(1+i4De^2\right)} \tag{14-b}$$

where $v_w^* = -1/\sqrt{DeRe}$.

Given the definition of ϕ and that the velocity must vanish as $y \to \infty$, it is necessary for the real part of the exponential appearing in the velocity profile (Equation 7) to be negative, i.e., the real part of $-zB$ must be negative. Given the expressions above and after some laborious mathematics carried out with MATHEMATICA v5 from Wolfram Research, the real and imaginary parts of $-zB$ are given by equations (15-a) and (15-b) or (16-a) and (16-b), respectively depending on the value of M_w. The solutions of Equation (15) are for the general case where $v_w^{*2} DeRe \neq 1$ (or $M_w \neq -1$)

$$(-zB)_{real} = \frac{\left\{ v_w Rea_1 + \sqrt{\mathrm{Re}}\varphi^{1/4}\left[a_2 + a_3 + a_4\right]\right\}}{\left(v_w^2 ReDe - 1\right)\left[a_5 + a_6 + a_7\right]} \tag{15-a}$$

$$(-zB)_{imag.} = \frac{-i\sqrt{Re}\left\{ m\left(1 + v_w^2 ReDe\right)a_8 + v_w\sqrt{Re}\left(a_9 + a_{10} + a_{11}\right)\right\}}{\left(v_w^2 ReDe - 1\right)\left[a_5 + a_6 + a_7\right]} \tag{15-b}$$

where

$$\varphi = v_w^4 Re^2 - 8v_w^2 ReDe + 16\left(1 + De^2\right) \text{ and } \theta = Arg\left[v_w^2 Re - 4De + 4i\right] = \arctan\left(\frac{4}{v_w^2 Re - 4De}\right)$$

with functions a_1 to a_{11} given below.

$$a_1 = -8 + v_w^2 Re\left(v_w^2 Re + 4De - 2\sqrt{\varphi}\right); \quad a_2 = -2mv_w^2 Re\left(v_w^2 Re + \sqrt{\varphi}\right)\cos\left(\frac{\theta}{2}\right); \quad a_3 = -v_w^3 Re^{3/2}\varphi^{1/4}\cos\theta$$

$$a_4 = -\left(1 + v_w^2 ReDe\right)\left[m\left(v_w^2 Re - 4De + \sqrt{\varphi}\right) + 2v_w\sqrt{Re}\varphi^{1/4}\cos\left(\frac{\theta}{2}\right)\right]\sin\left(\frac{\theta}{2}\right)$$

$$a_5 = v_w^4 Re^2 + 8 + 16De^2 + 2v_w^2 Re\sqrt{\varphi}\ ; \quad a_6 = 2mv_w\sqrt{Re}\left(v_w^2 Re + 4De + \sqrt{\varphi}\right)\varphi^{1/4}\cos\left(\frac{\theta}{2}\right)$$

$$a_7 = \left(v_w^2 Re + 4De\right)\sqrt{\varphi}\cos(\theta); \quad a_8 = \left(3v_w^2 Re + 4De + \sqrt{\varphi}\right)\varphi^{1/4}\cos\left(\frac{\theta}{2}\right)$$

$$a_9 = \left(1 + v_w^2 ReDe\right)\left(v_w^2 Re + 4De + 2\sqrt{\varphi}\right); \quad a_{10} = \left(1 + v_w^2 ReDe\right)\sqrt{\varphi}\cos\theta\ ;$$

$$a_{11} = 4De\varphi^{1/4}\left[2mv_w\sqrt{Re}\sin\left(\frac{\theta}{2}\right) + \varphi^{1/4}\sin\theta\right]$$

For the specific case of $v_w^{*2} DeRe = 1$ (or $M_w = M_w^* = -1$), the solutions of $(-zB)_{real}$ and $(-zB)_{imag}$ are given by

$$(-zB)_{real} = \frac{v_w \mathrm{Re}\left(6 + 25M^4 + 24M^8\right)}{\left(9 + 52M^4 + 64M^8\right)} \tag{16-a}$$

$$(-zB)_{imag} = -i\frac{5v_w Re^2 De}{\left(9 + 52M^4 + 64M^8\right)} \tag{16-b}$$

It is now possible to back-substitute some of the above equations to obtain the final expressions for the velocity and stress fields. For the velocity, the final equation takes the form

$$u = e^{-z\phi} \to u = e^{-z(At+By)} \to u = e^{(-zB)_{real}y} e^{i\left[t + (-zB)_{imag}y\right]} \tag{17}$$

where $e^{i\left[t+(-zB)_{imag}y\right]} = \cos\left[(-zB)_{imag}y + t\right]$ and $(-zB)_{real}$ and $(-zB)_{imag}$ are given by equations (15-a) and (15-b) for $M_w \neq 1$ and by equations (16-a) and (16-b) for $M_w = 1$, respectively.

4 Results and discussion

Some results of the previous section are discussed in detail here to investigate the role of the various relevant independent non-dimensional numbers. We start with the inspection of the Newtonian case and this is followed by an investigation of the viscoelastic flow in the absence of suction, since these two cases correspond to existing solutions in the literature. Then, the new results of this work are presented, the investigation of the viscoelastic flow with suction for low and large viscoelastic Mach numbers (M). Regardless of the elastic Mach number value, time imposed physical limit is by suction since the elastic suction Mach number (M_w) can not exceed 1 (in absolute value). This corresponds to suction velocity equal to the elastic wave speed. Of the two

solutions implied by equation (14-a), it was also found that only the solution corresponding to m= -1 was physically possible.

To help interpret the results two characteristic distances are defined: y_c is the normalized peak-to-peak distance of two consecutive oscillations and y_p is the normalized penetration depth, measuring the penetration of the oscillating wave. y_p is defined as the distance from the plate to the location where the maximum amplitude of fluid oscillation has been reduced to 1% of the amplitude of oscillation of the plate, so, it is equivalent to a boundary layer thickness. Those two quantities are given in equations (18) and (19), respectively.

$$y_c = \frac{2\pi}{(zB)_{imag}\dfrac{\omega}{U_0}} \tag{18}$$

$$y_p = \frac{-\ln(0.01)}{(-zB)_{real}} = \frac{4.6}{(-zB)_{real}} \tag{19}$$

4.1 Newtonian flow with a porous oscillating wall

Figs. 1-a) and 1-b) present velocity profiles for Newtonian fluids at Reynolds numbers of 1 and 10, respectively, in order to assess the combined effects of transverse velocity and Reynolds number in the absence of elasticity. All the profiles shown here and henceforth correspond to the moment when the oscillating plate is at the maximum amplitude of oscillation. This includes the situation with no suction ($v_w = 0$) of Stokes [10] and Lord Rayleigh [11]. For small suction velocities ($|v_w| \le 0.01$) the profiles of streamwise velocity are essentially unaffected by suction. As suction strengthens the penetration depth decreases, the streamwise velocity profiles approach the plate and the amplitude of fluid oscillation away from the plate is also reduced. This decrease of the amplitude of oscillation is associated with the larger streamwise shear stresses that develop when suction approaches the oscillating layers of fluid to each other and to the plate. However, the peak-to-peak distance y_c increases and consequently the ratio y_p / y_c decreases faster than the penetration depth as can be seen in Fig. 2. Note that the suction velocities are negative, i.e., suction increases from right to left in this figure.

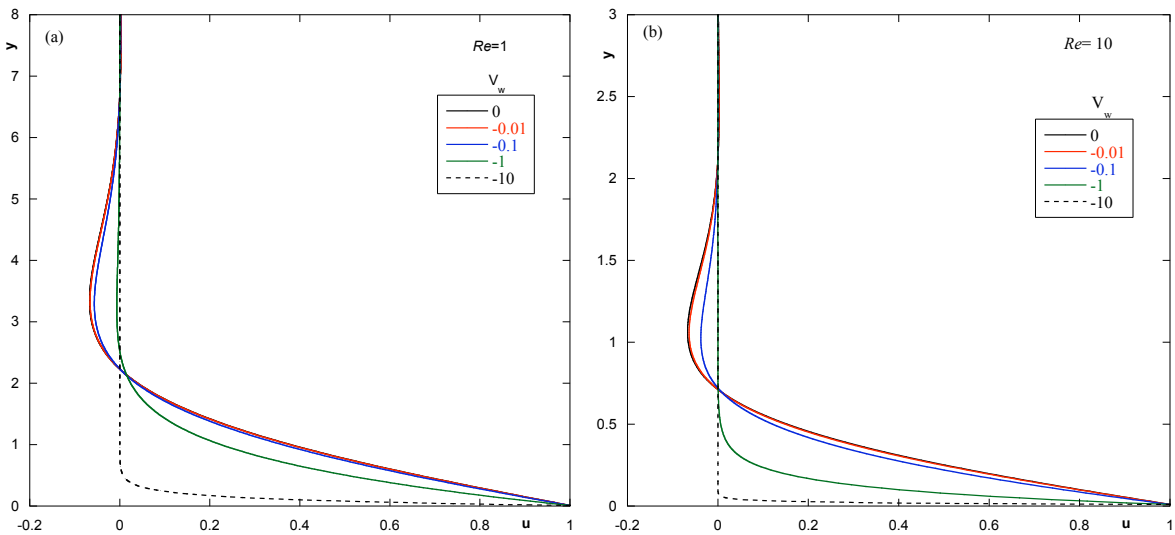

Fig. 1. Influence of Reynolds number and suction velocity through the porous wall on the streamwise velocity profiles for Newtonian fluids: (a) Re=1; (b) Re=10.

The comparison between Figs. 1-a) and 1-b) shows the Reynolds number effect on the velocity profiles. To understand this effect on the plot of u/U_0 versus $y\omega/U_0$ one is reminded that an increase in Reynolds number requires an increase in the amplitude of oscillation, a decrease in its frequency or both (apart from the effect of viscosity). Consequently, increasing the Reynolds number decreases the ordinate of the plot, $y\omega/U_0$, and the waves become compressed towards the plate, leading to higher shear rates and in spite of the reduction in the amplitude of the waves away from the wall.

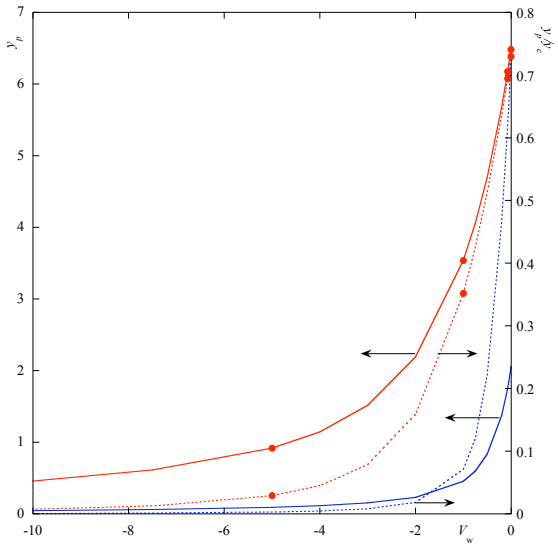

Fig.2. Variation of penetration depth (y_p) and of y_p/y_c with suction velocity for Newtonian fluids: red lines and circles Re= 1; blue lines Re= 10.

At *Re*= 1 the effect of the oscillating plate penetrates visibly to as much as *y*= 8 (c.f. Fig. 1-a), but this is significantly reduced on increasing the Reynolds number (at *Re*= 10 the fluid is almost at rest at *y*= 3, c.f. Fig.-1b), i.e., the penetration depth decreases on inverse proportion to *Re*. This is clear in Fig. 2 and the variation of y_p with Reynolds number is non-linear due to the effect of the suction velocity as will become clear in the next section. Here, it suffices to notice that the variation in y_p at v_w=0 is by a factor of 3 and increasing to a factor of 10 as $v_w \to -\infty$, whereas the Reynolds number variation is always from 1 to 10. In contrast, the peak-to-peak distance increases with suction velocity. Since y_c is always larger than the penetration depth, only a single cycle, or part of it, is actually seen in Fig. 1. At v_w=0 and infinite suction y_p/y_c becomes independent of Reynolds number.

The shear stress profiles are in agreement with the corresponding velocity profiles of Fig. 1 as far as the effects of *Re* and v_w are concerned, taking into account that they are proportional to the velocity gradient, and so are not shown here for conciseness.

4.2 Viscoelastic flow with an impermeable oscillating wall

The second reference case pertains to viscoelastic fluid flows in the absence of suction, the solution of which can be found elsewhere [3,4]. The corresponding streamwise velocity profiles at the same Reynolds numbers of 1 and 10, and showing the effects of Deborah number, are plotted in Figs. 3-a) and 3-b), respectively. For *De* ≤ 0.01, cases here corresponding to *M* << 1, there are hardly detectable differences relative to the Newtonian profiles. On further increasing the Deborah number, or elastic Mach number, two different characteristics become obvious. First, the shape of the velocity profile progressively evolves from that of a diffused wave at low elastic Mach numbers towards a less dampened wave containing more and more visible cycles at large Mach numbers. At low Reynolds numbers, as for *Re*=1 in Fig. 3-a), it looks as though this change of behavior is associated with the transition from sub-critical to super-critical flow, but comparison with Fig. 3-b) for *Re*= 10 shows that the elastic Mach number is not the critical parameter (the curve for *M*=1 at *Re*= 1 looks like the curve for *M*= 3.2 at *Re*= 10 in spite of the ordinate difference). In fact, inspection of Fig. 4-a), where the penetration depth and the ratio y_p/y_c are plotted as a function of Deborah and Reynolds numbers, shows that y_p/y_c is actually independent of Reynolds number at least here in the absence of suction, and only depends on the Deborah number.

The amplitude of the oscillating wave is also progressively less rapidly dampened on moving away from the plate and consequently the penetration depth of the wave increases. Simultaneously, the shear wave speed (*c*) and the peak-to-peak distance (y_c) of the traveling wave decrease with *De* and more and more cycles become visible.

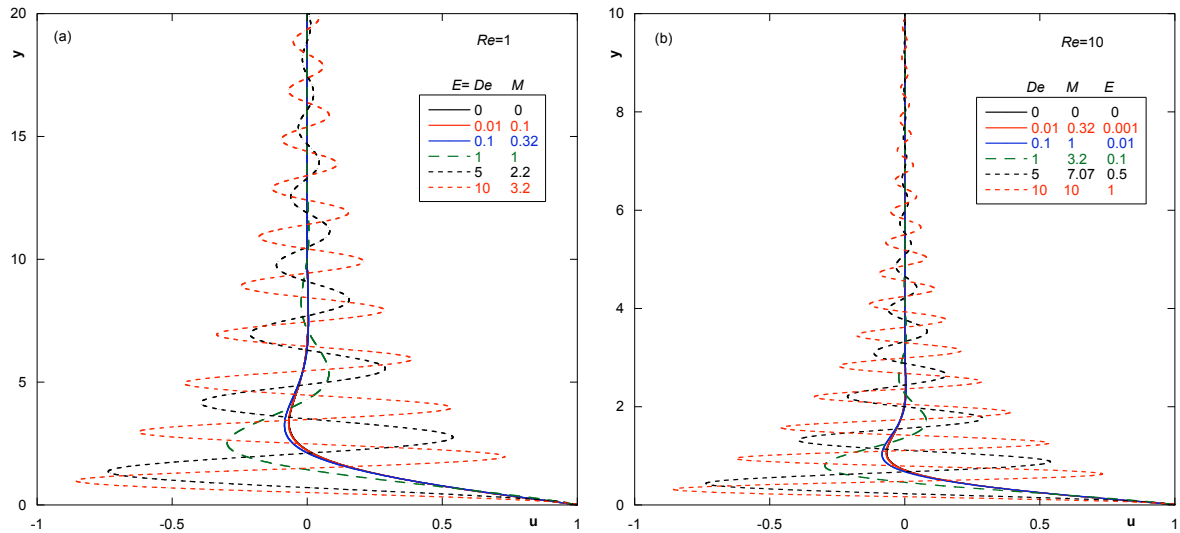

Fig. 3. Influence of Reynolds and Deborah numbers on the velocity profiles in the absence of suction: (a) *Re*= 1; (b) *Re*= 10.

Note that the fluid velocity is normalized by the amplitude of the plate velocity oscillation, so any change in this amplitude should not affect the plotted velocity, other factors being equal. The evolution of the wave behavior with *De* is also characteristic of an evolution from liquid-like to solid-like behavior or from the propagation of a viscous wave to the propagation of an elastic wave.

The effect of Reynolds number is now clarified. In the absence of suction, the waves become more persistent on account of elasticity and its effect in reducing the wave propagation speed and this is well seen in the increase of y_p with *De* shown in Fig. 4-a). However, in contrast to the suction velocity of the previous sub-section, the Deborah number does not change the impact of Reynolds number in a non-linear manner. A plot of $y_p\sqrt{Re}$ versus *De* in Fig. 4-b) collapses the penetration data pertaining to different Reynolds numbers. The same happens with the peak-to-peak distance and that explains the Reynolds number independence of y_p/y_c .

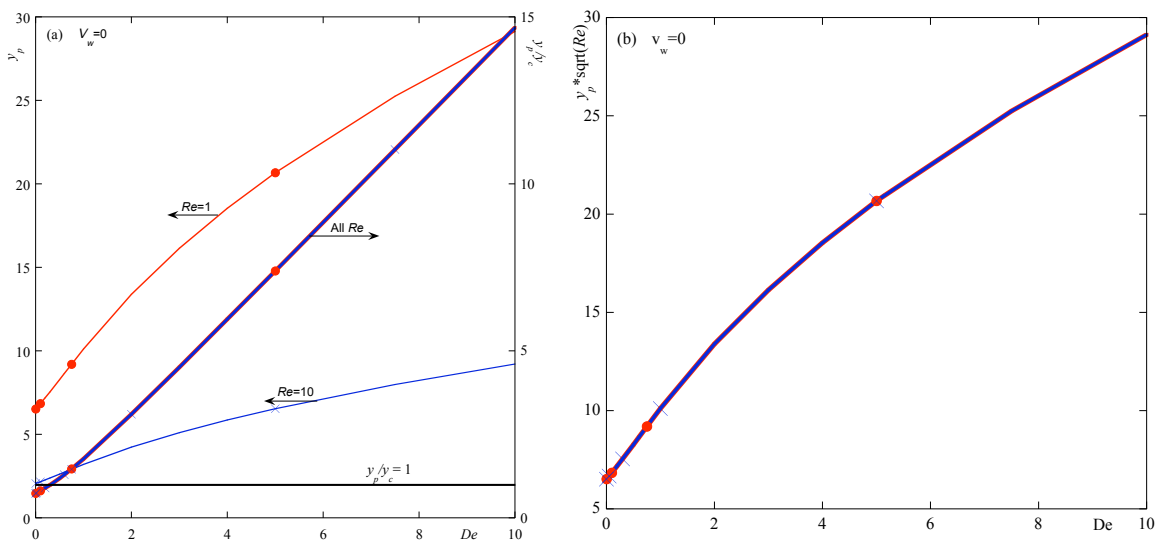

Fig. 4. Variation of characteristics depths with Deborah number in the absence of suction: red lines and circles *Re*= 1; blue lines and crosses *Re*= 10: (a) y_p and y_p/y_c ; (b) $y_p\sqrt{Re}$.

4.3 Viscoelastic flow with suction through the porous oscillating wall

The two plots of Fig. 5 are for a constant Reynolds number of 1 and increasing Deborah numbers of 0.1 and 1, respectively. Within each plot the suction velocity is varied, but no solution is ever obtained for $|M_w|>1$, i.e. when the suction velocity exceeds the wave speed. For $M_w=-1$ the suction velocity equals the wave speed so

only the fluid particles attached to the plate move in the streamwise direction and elsewhere the streamwise velocity is zero (but not the normal velocity which is equal v_w).

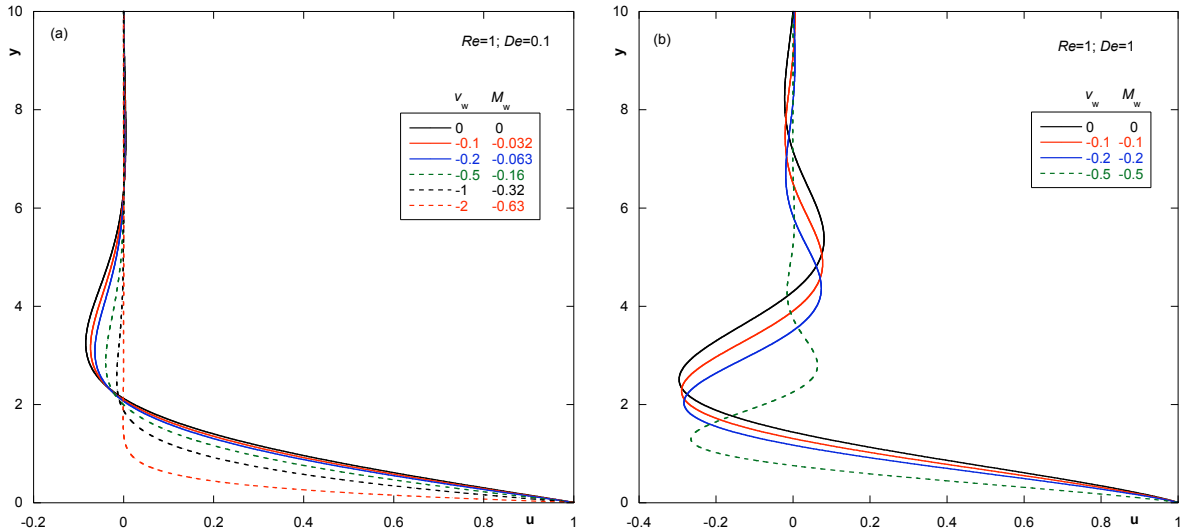

Fig. 5. Effect of suction velocity through the porous plate on the velocity profiles for *Re*= 1: (a) *De*= 0.1 (*M*= 0.32 and *E*= 0.1); (b) *De*= 1 (*M*= 1 and *E*= 1);

The first plot of Fig. 5 pertains to a subcritical Mach number ($M < 1$) and Fig. 5-b) is for $M = 1$. The effects of Deborah number are those expected from the findings of the previous section, but now combined with suction. Accordingly, the streamwise velocity profiles are dampened very quickly on moving away from the wall and the streamwise velocity vanishes essentially after one full period of oscillation. For *M*= 1, the amplitude of the oscillation is stronger and at *y*= 10 the oscillation is still clear, although weak. The reduction in the rate of decrease in the amplitude of oscillation with suction due to elasticity increases is especially well shown in the comparison between Figs. 5 –a) and 5-b).

The three plots of Fig. 6 are for a higher constant value of the Reynolds number of 10 and the Deborah numbers are now 0.1, 1 and 10 to simultaneously allow comparison with the results of Fig. 5, as well as to reach hypercritical elastic Mach numbers ($M > 5$). The effects of Reynolds number are also akin to those observed in Figs. 1 and 3, now in combination with suction and Deborah number. As for *Re*=1, $M_w = -1$ marks the limit of physical solutions when there is suction. Since the Reynolds number is now higher than in **Figure 5**, the profiles are closer to the wall.

The plot of Fig. 6-c) is for a very large elastic Mach number ($M = 10$) and shows well that the wave behavior is now largely dominated by fluid elasticity rather than viscous effects with several cycles in evidence especially when suction is weak.

The penetration depth and ratio y_p / y_c are plotted for *Re*= 1 and *Re*= 10 in Figs. 7-a) and 7-b), respectively, as a function of the elastic suction Mach number. The behaviours are non-linear, but the plot suggests that these quantities tend to behave linearly with M_w as the Deborah number increases and the flow becomes dominated by elasticity.

Another important and unexpected finding is shown in Fig. 8 and confirms a result obtained without suction, namely that the penetration depth and the peak-to-peak distance scale with $1/\sqrt{Re}$, even in the presence of combined effects of elasticity and suction. For conciseness only the plots of $y_p\sqrt{Re}$ at two different Deborah numbers are shown. So, even though the analytical solution is somewhat complex, there are simple scaling laws for this complex viscoelastic flow.

The increased penetration depth of the oscillations is consistent with findings in turbulent flow of viscoelastic fluids where the damping effect of walls in reducing turbulence is seen to have a longer range of action than for Newtonian fluids. Therefore, this solution can inspire the development of Van Driest type of damping functions for turbulence of drag reducing fluids.

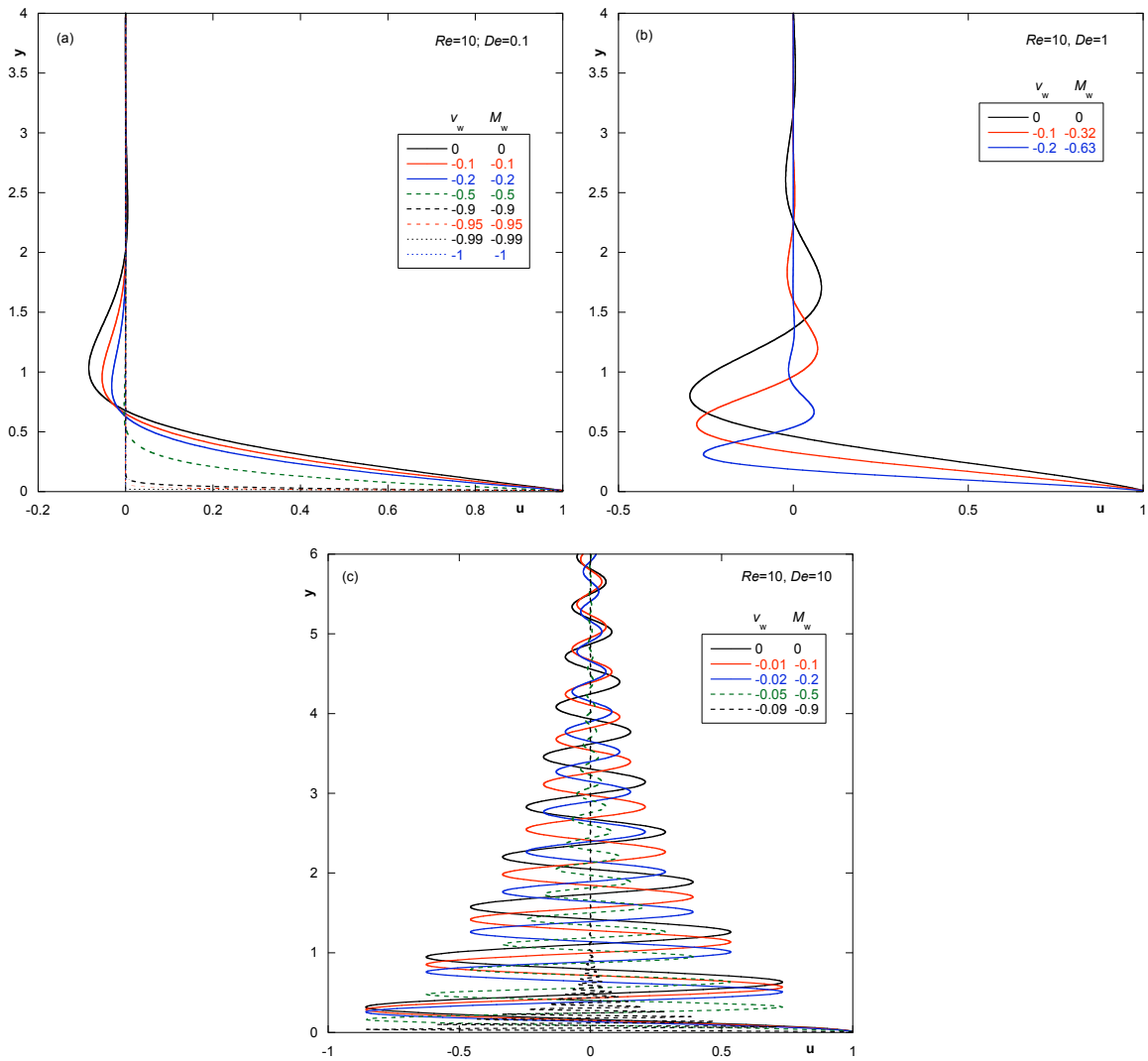

Fig. 6. Effect of suction velocity through the porous plate on the velocity profiles for *Re*= 10: (a) *De*= 0.1 (*M*= 1 and *E*= 0.01); (b) *De*= 1 (*M*= 3.2 and *E*= 0.1); (c) *De*= 10 (*M*= 10 and *E*= 1).

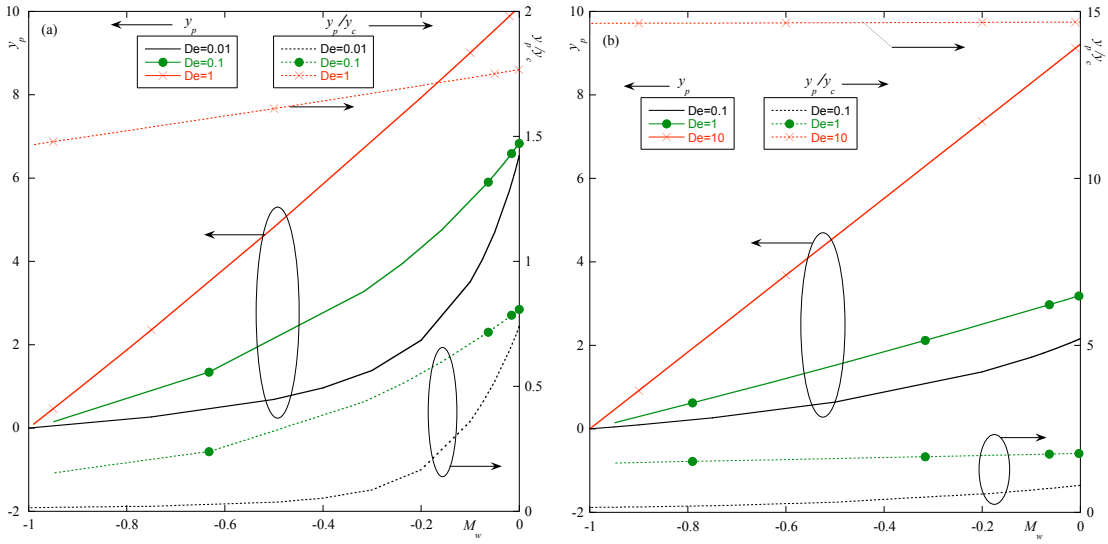

Fig. 7. Variation of penetration depth (full line) and y_p/y_c (dashed line) with elastic suction Mach number and Deborah number: (a) *Re*= 1; (b) *Re*= 10.

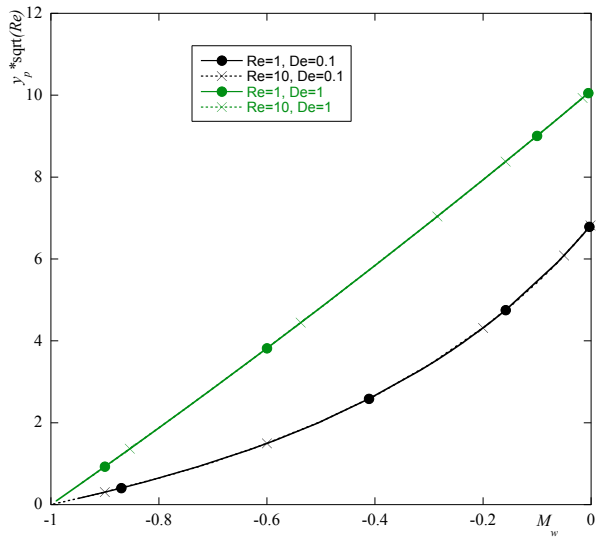

Fig. 8. Variation of $y_p\sqrt{Re}$ with suction elastic Mach number and Deborah number.

5 Conclusions

An analytical solution was derived for the time-dependent flow of an infinite pool of UCM fluid driven by the oscillation of a porous plate through which there is suction. In contrast to the Newtonian case, for viscoelastic fluids physical solutions require the suction velocity not to exceed the elastic wave speed. Suction pushes the oscillating fluid towards the plate, but as the Deborah number increases the waves become dominated by elasticity, dampening of the oscillations is reduced, especially at large elastic Mach numbers and the penetration depth increases. In spite of the elaborate solution and the complex interaction between *Re*, *De* and suction, simple scaling laws were found for $y_p\sqrt{Re}$ and y_p/y_c which are independent of *Re*.

Acknowledgments

F. T. Pinho gratefully acknowledges funding from FEDER and FCT through Projects POCI/56342/EQU/2004 and PTDC/EME-MFE/70186/2006 and D. O. A. Cruz would like to thank CNPq Project number 304865/2005-2 for financial support.

References

1. P. J. Oliveira, Method for time-dependent simulations of viscoelastic flows: vortex shedding behind cylinder. *J. Non-Newt. Fluid Mech.*, 101, 113-137, 2007.
2. R. B. Bird, R. A. Armstrong and O. Hassager, *Dynamics of Polymeric Liquids*. *Vol I: Fluid Dynamics.*, John Wiley and Sons, New York, 1987.
3. T. Hayat, A. M. Siddiqui and S. Ashgar, Some simple flows of an Oldroyd-B fluid. *Int. Journal of Engineering Science*, 39, 135-147, 2001.
4. N. Aksel, C. Fetecau and M. Scholle, Starting solutions for some unsteady unidirectional flows of Oldroyd-B fluids. *Z. Angew. Math. Phys.*, 57, 815-831, 2006.
5. N. D. Waters and M. J. King, Unsteady flow of an elastico-viscous liquid. *Rheol. Acta*, 9, 345-355, 1970.
6. Y. Mochimaru, Unsteady-state development of plane Couette flow for viscoelastic fluids. *J. Non-Newt. Fluid Mechanics*, 12, 135-152, 1983.
7. R. I. Tanner, Note on the Rayleigh problem for a viscoelastic fluid. *Z. Angew. Math. Phys.*, 13, 573-580, 1962.
8. M. E. Erdogan, A note on an unsteady flow of a viscous fluid due to an oscillating plane wall. *Int. Journal of Engineering Science*, 35, 1-6, 2000.
9. D. D. Joseph, *Fluid Dynamics of Viscoelastic Liquids*. Volume 84 of Applied Mathematical Sciences Series, Springer Verlag, Berlin, 1990.
10. G. G. Stokes, On the effect of the internal friction of fluids on the motion of pendulums. *Trans. Cambr. Phil. Soc.*, 9, Part II, 8-106, 1856.
11. Lord Rayleigh, On the motion of solid bodies through viscous liquids. *Phil. Mag.*, 20 , 697-711, 1911.